JOURNAL OF DIFFERENCE EQUATIONS AND APPLICATIONS
2022, VOL. 28, NO. 10, 1268–1281
https://doi.org/10.1080/10236198.2021.1972986

Bifurcation analysis of a piecewise-smooth Ricker map with proportional threshold harvesting

Eduardo Liz

Departamento de Matemática Aplicada II, Universidade de Vigo, Vigo, Spain

ABSTRACT

Proportional threshold harvesting (PTH) refers to some control rules employed in fishing policies, which specify a biomass level below which no fishing is permitted (the threshold), and a fraction of the surplus above the threshold is removed every year. When these rules are applied to a discrete population model, the resulting map governing the harvesting model is piecewise smooth, so border-collision bifurcations play an essential role in the dynamics. In this paper, we carry out a bifurcation analysis of a PTH model, providing a thorough picture of the 2-parameter bifurcation diagram in the plane (T, q) for a case study. Here, T is the threshold and q is the harvest proportion. Our results explain some numerical bifurcation diagrams in previous work for PTH, and uncover new features of the dynamics with interesting consequences for population management.

ARTICLE HISTORY
Received 18 May 2021
Accepted 23 August 2021

KEYWORDS
Piecewise-smooth maps; border-collision bifurcations; threshold harvesting; Ricker map

MATHEMATICS SUBJECT CLASSIFICATIONS
39A28; 92D25

1. Introduction

Discrete dynamical systems constitute a very useful mathematical description of population models, especially when reproduction occurs only once a year, during a short season [12,20]. In particular, they are widely used in fisheries, where the so-called stock-recruitment function governs the between-year dynamics [4,18]. In this context, it is very important to investigate how different management policies influence population dynamics.

Fisheries have to find a balance between maximizing the yield and minimize the risk of extinction. This aim leads to use fishing strategies based on biological reference points, such as target fishing mortality or threshold biomass levels [17]. Recently, many fisheries have adopted threshold control rules in their harvest policies to ensure that populations are not overfished. These rules specify a biomass level below which no fishing is permitted (the threshold), and different forms of harvesting (constant, proportional) are applied otherwise [5,13,16].

Theoretical methods based on the use of population models are an essential tool to estimate and evaluate the choice of suitable reference points as well as the response of fisheries to different forms of threshold harvesting [19]. In particular, discrete-time dynamical

CONTACT Eduardo Liz eliz@uvigo.es, eliz@dma.uvigo.es Departamento de Matemática Aplicada II, Universidade de Vigo, Vigo 36310, Spain

systems have been recently used for this purpose; for example, 'pure' threshold harvesting (the entire excess of a population stock above the threshold level is removed) was studied in [10], different forms of threshold constant-catch harvesting (a fixed quota is removed if population stock is above the threshold) can be found in [1,11,15], and proportional threshold harvesting (a fraction of the population surplus above the threshold is removed) was addressed in [3,8,9].

Consider a discrete population model in the form

$$x_{n+1} = f(x_n), \tag{1}$$

where x_n denotes the population at the nth generation and f is the reproduction (stock-recruitment) function. In a natural way, when threshold harvesting is applied to (1), the resulting dynamical system is governed by a piecewise-smooth map. Thus, the study of such maps [2,6] became an essential tool to understand the dynamics of threshold harvesting population models, as pointed out by Bischi et al. [3] (see also [11,15]).

In the recent paper [9], we studied how the stability properties of the positive equilibrium depend on the threshold parameter for a family of discrete-time population models subject to proportional threshold harvesting (PTH). If in the absence of harvesting the population abundance in a year in terms of the population at the previous year is governed by (1), the harvesting model is given by the difference equation

$$x_{n+1} = G(x_n) := \begin{cases} f(x_n) & \text{if } f(x_n) \le T, \\ F(x_n) := f(x_n) - q(f(x_n) - T) & \text{if } f(x_n) > T. \end{cases} \tag{2}$$

where $q \in (0, 1]$ is the harvest proportion and T is the threshold.

In the limit case $q = 1$, (2) becomes the pure threshold harvesting rule (TH), defined by the map $G_1(x) = \min\{f(x), T\}$. The limit case $T = 0$ gives the usual proportional harvesting (PH) method, defined by the map $G_2(x) = (1 - q)f(x)$ (see, e.g. [14]).

One of the main conclusions of [9] is that increasing harvesting by decreasing the threshold can have different effects on the stability of the equilibrium, depending on the considered function f. In particular, for the Ricker map $f(x) = x\, e^{r(1-x)}$, increasing harvesting intensity by decreasing the threshold T is destabilizing for a range of q values. We have also observed numerically that bistability can occur for some combinations of the two relevant parameters T and q.

Since the map G defined in (2) is piecewise-smooth, border-collision bifurcations (BCBs) [2,6] play an essential role in the dynamics. In this paper, we carry out a bifurcation analysis of (2), providing a thorough picture of the 2-parameter bifurcation diagram in the plane (T, q) for a case study. We choose the Ricker model with $r = 2.6$, for which the unique attractor is 4-periodic. With this choice, on the one hand we avoid chaotic dynamics that would obscure the influence of BCBs; on the other hand, the cyclic dynamics highlights how the combination of border-collision and smooth bifurcations (SBs) enriches the dynamics.

The results in this paper explain some numerical bifurcation diagrams in previous work for PTH [8,9]. Our main findings are the following:

- We describe all possible bifurcations (BCBs and SBs) for our case study;

- we identify the regions of bistability in the 2-parameter bifurcation diagram and the mechanisms that create or destroy bistability;
- we determine the period (1, 2 or 4) of the attractors, both in the regions where there is a unique attractor or where bistability occurs;
- we show a sort of robustness of the limit cases: when T is the bifurcation parameter, we demonstrate that for large enough values of q (q close to 1), the dynamics of (2) are similar to those of the limit case $q = 1$ (TH). If q is the bifurcation parameter, then the dynamics of (2) for small values of T is similar to the dynamics of the limit case $T = 0$ (PH);
- we distinguish between observable and non-observable bifurcations. The latter correspond to persistence BCBs between unstable cycles;
- we identify the mechanisms that lead to subcritical or supercritical flip BCBs.

2. Preliminaries

In the following, we focus on the Ricker model, that is, we consider Equation (2) with $f(x) = x\,e^{r(1-x)}$, which we state below for later reference.

$$x_{n+1} = G(x_n) := \begin{cases} f(x_n) := x_n\, e^{r(1-x_n)} & \text{if } f(x_n) \le T, \\ F(x_n) := (1-q)x_n\, e^{r(1-x_n)} + qT & \text{if } f(x_n) > T. \end{cases} \tag{3}$$

From now on, we assume that $r > 2$ because for $r \le 2$ the dynamics of (3) are trivial: all solutions converge to 1 if $T \ge 1$, and all solutions converge to the unique positive fixed point $p \in (T, 1)$ of F if $T < 1$ [9, Propositions A.3 and A.4].

We follow [6] for notations related to piecewise-smooth maps and border-collision bifurcations, see also [2].

The map G has a unique positive equilibrium p [9, Proposition A.1]. If $T \ge 1$, then the positive equilibrium is $p = 1$, which is the positive fixed point of f; moreover, if $T > 1$ then $G'(1) = f'(1) = 1 - r < -1$, and therefore p is unstable. If $T < 1$, then 1 is not a fixed point of G. In terms of [6], 1 is an admissible fixed point of G if $T \ge 1$, and a virtual fixed point if $T < 1$. When $T = 1$, we say that 1 is a boundary fixed point of G, which means that G is not differentiable at the fixed point $p = 1$. For the map F, the opposite occurs: if $T > 1$, then the unique positive fixed point of F, $p \in (1, T)$, is a virtual fixed point of G, and $p \in (T, 1)$ is admissible if $T < 1$.

If we choose T as the bifurcation parameter, a BCB occurs at $T = 1$. In our case, only two types of BCBs for fixed points can occur:

- A *persistence BCB* occurs at $T = 1$ when an admissible and a virtual fixed point collide and interchange their roles. No other periodic points are created or destroyed at the bifurcation point.
- A *flip BCB* or *period-doubling BCB* occurs at $T = 1$ when a 2-periodic orbit $\{p_1, p_2\}$ of G is created either for $T \in (1 - \varepsilon, 1)$ or for $T \in (1, 1 + \varepsilon)$, for some $\varepsilon > 0$, where p_1 and p_2 are at different sides of the boundary fixed point (that is, $F(p_1) = p_2, f(p_2) = p_1$). See Figure 1 for an illustration.

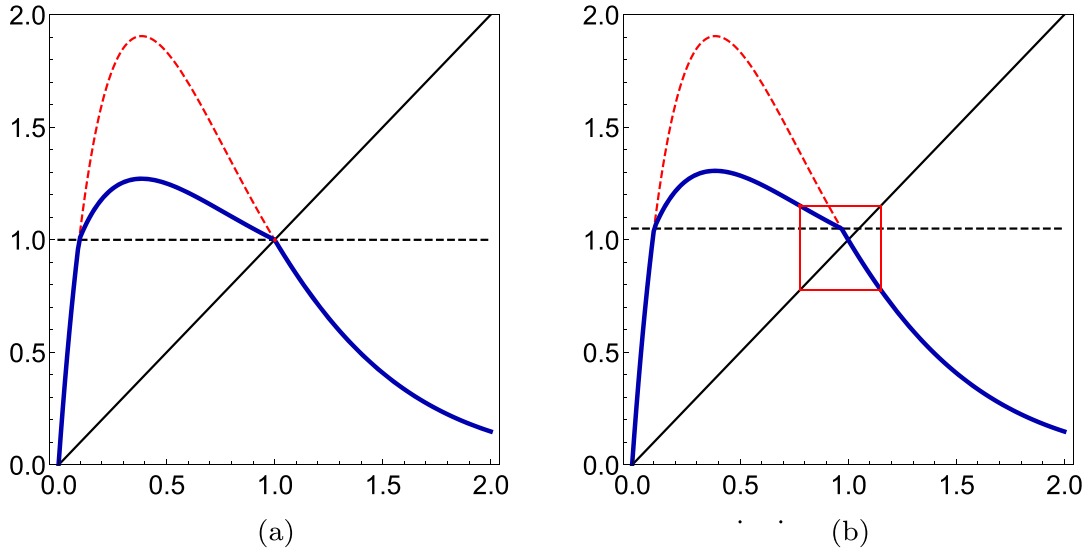

Figure 1. Detail of a supercritical flip BCB in (3), with $r = 2.6$, and $q = 0.7$, as T is increased and passes the critical value $T = 1$. The graph of G is represented by the blue, solid curve; the red dashed curve corresponds to the graph of f, and the black dashed line represents the threshold. (Colours refer to the online version). (a) The fixed point $p = 1$ is an attractor of (3) for $T = 1$. (b) A 2-periodic attractor of (3) for $T = 1.05$.

Following [6], we denote a stable admissible fixed point of F by the letter A, an unstable admissible fixed point of F by a, a stable admissible fixed point of f by B, and an unstable admissible fixed point of f by b. A period-two point of G is denoted by AB if it is stable and ab otherwise. We use the symbol $\leftrightarrow$ to indicate the occurrence of a BCB as T passes through 1. Using this notation, we distinguish between non-observable persistence BCBs ($a \leftrightarrow b$) and observable persistence BCBs ($A \leftrightarrow B$). Clearly, the former do not have any influence in the observable dynamics. Also, we distinguish between a supercritical flip BCB ($A \leftrightarrow \{b, AB\}$) and a subcritical flip BCB ($\{A, ab\} \leftrightarrow b$). We use the classification criteria in [6, Theorem 3.1 and Figure 3.5] to identify the type of BCBs for fixed points in the next section.

We also find in our case study BCBs for fixed points of the second iteration G^2 and the fourth iteration G^4 of G, that is, for the 2-periodic and 4-periodic orbits of G. These BCBs can be of the same type as the previous ones, but there are fold BCBs as well. For example, a fold BCB for G^2 takes place when an attracting and a repelling 2-periodic orbits collide and then disappear ($\{ab, AB\} \leftrightarrow \emptyset$). This border collision occurs when $F(F(T)) = T$.

3. Bifurcations

In this section, we describe all possible smooth and border-collision bifurcations in (3) with $r = 2.6$, using either T or q as bifurcation parameters, which allows us to represent a 2-parameter bifurcation diagram in Figure 2. It is well known that, as r grows, the Ricker map undergoes a period-doubling bifurcation sequence to chaos, so its dynamics become complex for r large enough. It is expected that the dynamics of (3) will be more complicated as well, in particular exhibiting multiple bistability regions in the 2-parameter bifurcation

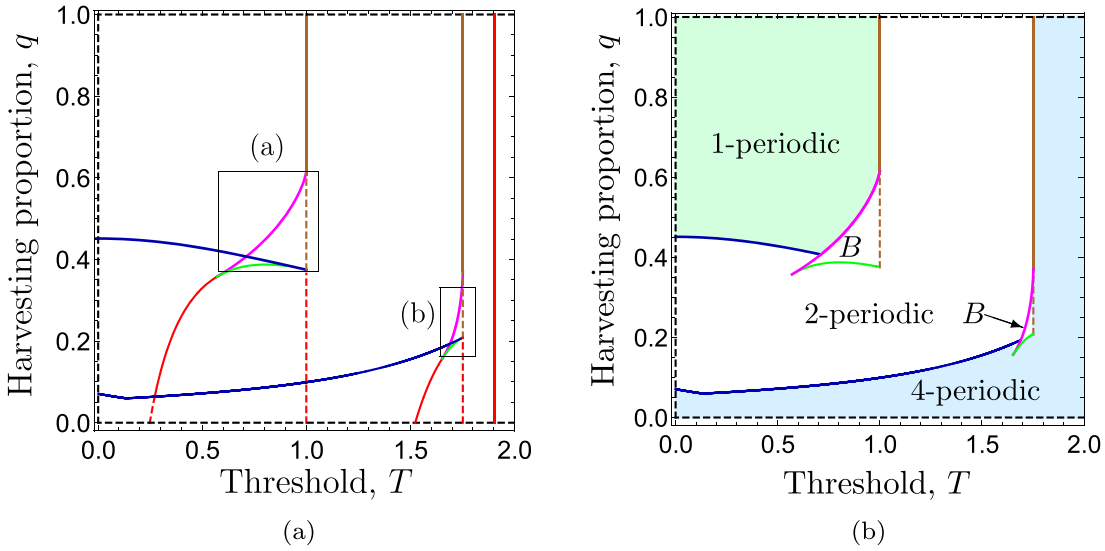

Figure 2. Two representations of the 2-parameter bifurcation diagram for (3) with $r = 2.6$, showing smooth and border-collision bifurcation boundaries, as well as the location of periodic attractors. For a zoom of the bistability regions, see Figure 3. (a) Smooth and border-collision bifurcation boundaries. See the text for a detailed explanation of the different colours, which refer to the online version. (b) Regions with periodic attractors of period 1, 2 or 4. There is bistability in the two regions marked with B.

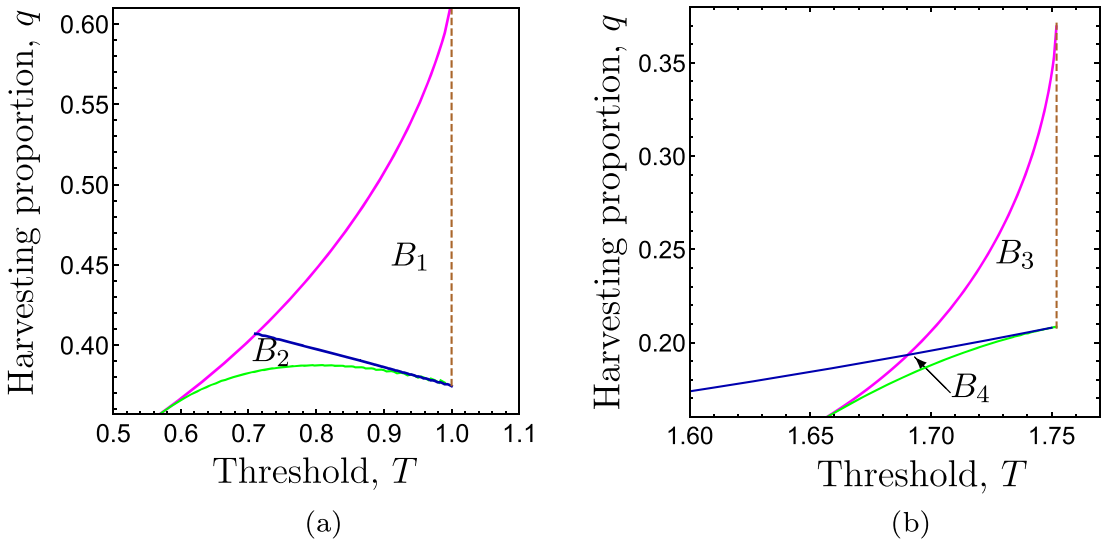

Figure 3. Zoom of the bistability regions corresponding to the boxes in Figure 2 (a). (a) Coexistence between a fixed point and a 2-cycle (B_1), and between two 2-cycles (B_2). (b) Coexistence between a 2-cycle and a 4-cycle (B_3), and between two 4-cycles (B_4).

diagram. However, our simulations for other values of r suggest that the main changes in the dynamics due to border-collision bifurcations are very similar to those appearing in the case $r = 2.6$.

We begin with smooth bifurcations, and then we study BCBs, which are divided in bifurcations of fixed points, of 2-periodic cycles, and of 4-periodic cycles.

3.1. Smooth bifurcations

We find flip and fold smooth bifurcations. A flip bifurcation occurs when $T < 1$ and $F'(p) = (1-q)f'(p) = -1$, where p is the positive fixed point of F. For $T \geq 1$, the unique positive equilibrium of G is 1, and it is unstable. This bifurcation has been studied in [9], and defines a decreasing smooth curve in the 2-parameter plane (T, q) (for an implicit equation of the curve, see [9, Proposition A.5]). We emphasize that this is the only bifurcation curve for (3) studied in [9]. All results from here are new.

Let $x = T^* \approx 1.752$ be the unique solution $x > 1$ of equation $x = f^2(x)$. A second flip bifurcation occurs when $T < T^* \approx 1.752$ and an attracting 2-cycle $\{p_1, p_2\}$ of G satisfies $G^2(p_1) = p_1$, $(G^2)'(p_1) = -1$. For $T \geq T^*$, the unique 2-periodic orbit of G is $\{T^*, f(T^*)\}$, and it is unstable.

These flip SBs are represented in Figure 2 by blue solid lines. It is worth emphasizing that the second one defines a continuous curve in the 2-parameter plane (T, q), but it is not differentiable at $T = T_\# \approx 0.1346$. The reason is that for $T < T_\#$ the equations defining the bifurcation are $F^2(p_1) = p_1$, $(F^2)'(p_1) = -1$, while for $T > T_\#$ they are given by $f(F(p_1)) = p_1, f'(F(p_1))F'(p_1) = -1$, where $p_1 < 1$.

The map G has always a unique positive fixed point, and therefore there are no fold bifurcations for G. However, we find fold bifurcations for G^2 and G^4. In both cases, the corresponding bifurcation curve is represented in Figure 2 by a magenta solid line (see the zoom in Figure 3).

The fold SB for G^2 is defined, for $T < 1$, by the system $f(F(x)) = x, f'(F(x))F'(x) = 1$. Two periodic orbits (one attracting and one repelling) appear at the bifurcation curve as T increases or q decreases. This bifurcation curve is defined for $T \in (\tilde{T}, 1)$, where $\tilde{T} \approx 0.5709$. At this point, the curve collides with a branch of fold BCBs ($F^2(\tilde{T}) = \tilde{T}$).

Similarly, a fold SB for G^4 is defined, for $T \in (1, T^*)$, by the system $H(x) = x, H'(x) = 1$, where $H(x) = F(f(f(f(x))))$. In this case, two 4-periodic orbits (one attracting and one repelling) appear as T increases or q decreases and meet the bifurcation curve. This bifurcation curve is defined for $T \in (\overline{T}, T^*) \approx (1.653, 1.752)$. At $T = \overline{T}$, the curve collides with a branch of fold BCBs ($(F \circ f)^2(\overline{T}) = \overline{T}$).

3.2. Border-collision bifurcations

Next, we describe all possible BCBs in (3) using either T or q as bifurcation parameters. We distinguish BCBs for fixed points, 2-periodic orbits and 4-periodic orbits.

3.2.1. BCBs of fixed points

BCBs of fixed points only occur at $T = 1$, when $F(T) = f(T) = T$. In the next proposition, we give the precise classification of the different types of BCBs that occur as the bifurcation parameter T meets the critical value $T = 1$. In particular, this result explains the numerical bifurcation diagrams in [9, Figure 6].

Proposition 3.1: *Assume that $r > 2$. Then Equation* (3) *undergoes a BCB as T meets the critical value $T = 1$. This BCB is:*

- *a flip BCB if $1 > q > (r-2)/(r-1)$;*
- *a persistence BCB if $0 < q < (r-2)/(r-1)$.*

Moreover, the flip BCB is supercritical if $q \in ((r-2)/(r-1), r(r-2)/(r-1)^2)$ *and subcritical if* $q > r(r-2)/(r-1)^2$.

Proof: Following the terminology in [6, Theorem 3.1], we denote by σ_1^+ (resp. σ_1^-) the number of real eigenvalues greater than 1 (resp. the number of real eigenvalues less than -1) of the linearization $G'(1^-) = F'(1)$. Analogously, we denote by σ_2^+ (resp. σ_2^-) the number of real eigenvalues greater than 1 (resp. the number of real eigenvalues less than -1) of the linearization $G'(1^+) = f'(1)$.

In addition, σ_{11}^+ and σ_{12}^+ are the number of real eigenvalues of $F'(1)F'(1)$ and $F'(1)f'(1)$ which exceed 1, respectively.

Thus, the relevant values to classify the BCBs at $T = 1$ are $f'(1)$, $F'(1) = (1-q)f'(1)$, $F'(1)f'(1) = (1-q)(f'(1))^2$, and $F'(1)F'(1) = (1-q)^2(f'(1))^2$.

We easily get:

- $\sigma_1^+ = \sigma_2^+ = 0$ (because $f'(1) = 1 - r < 0$);
- $\sigma_2^- = 1$ (because $f'(1) = 1 - r < -1$);
- $\sigma_1^- = 1$ if $(1-q)f'(1) < -1$, and $\sigma_1^- = 0$ if $(1-q)f'(1) > -1$.

Hence, if $(1-q)f'(1) < -1$, then $\sigma_1^- + \sigma_2^-$ is even, and thus there is a persistence BCB, of the form $a \leftrightarrow b$. This condition is equivalent to $q < (r-2)/(r-1)$.

If $q > (r-2)/(r-1)$, then $(1-q)f'(1) > -1$ and $\sigma_1^- + \sigma_2^-$ is odd. Hence, there is a flip BCB. The character of this bifurcation depends now on σ_{11}^+ and σ_{12}^+. Since $0 > F'(1) = (1-q)f'(1) > -1$, it follows that $F'(1)F'(1) = (1-q)^2(f'(1))^2 < 1$, and therefore $\sigma_{11}^+ = 0$. This means that the bifurcation is supercritical ($A \leftrightarrow \{b, AB\}$) if $\sigma_{12}^+ = 0$, which is equivalent to $(1-q)(f'(1))^2 < 1$, and it is subcritical ($\{A, ab\} \leftrightarrow b$) if $\sigma_{12}^+ = 1$, which is equivalent to $(1-q)(f'(1))^2 > 1$. Thus, the flip BCB is subcritical for $q \in ((r-2)/(r-1), r(r-2)/(r-1)^2)$, and it is supercritical if $q > r(r-2)/(r-1)^2$). ■

For $r = 2.6$, we get a persistence BCB for each $q < 0.375$, a subcritical flip BCB for $q \in (0.375, 0.609375)$, and a supercritical flip BCB for $q > 0.609375$.

See Figure 1 for an illustration of a supercritical flip bifurcation for $q = 0.7 > 0.609375$.

The bifurcation boundaries corresponding to the case $T = 1$ are represented by vertical lines in Figure 2: brown solid line for flip supercritical, brown dashed line for flip subcritical, and red dashed line for persistence (notice that it is non-observable because the involved equilibria are unstable).

3.2.2. BCBs of 2-periodic cycles

When a fixed point of G^2 collides with T, a border-collision bifurcation occurs. In our context, there are two possibilities: either $T = f^2(T)$, with $T > 1$, or $T = F^2(T)$, with $T < 1$.

Recall that $T^* \approx 1.752$ satisfies $f^2(T^*) = T^*$. The classification of BCBs that occur as the bifurcation parameter T meets the critical value T^* can be made in an analogous way to the previous case ($T = 1$). We provide the classification but skip the details.

If $q < q_1 \approx 0.208$, then there is a (non-observable) persistence BCB: two unstable 2-periodic orbits switch from admissible to virtual periodic points of G^2. The value q_1 is found solving (numerically) equation $(F \circ f)'(T^*) = -1$.

If $q_1 < q < q_2 \approx 0.3735$, then there is a subcritical flip BCB for G^2. This means that, as T is increased and passes through T^*, an unstable 4-periodic orbit and an attracting 2-periodic orbit collide. For $T > T^*$, an unstable 2-cycle of f becomes an admissible cycle of G. The value q_2 is found solving (numerically) equation $(F \circ f^3)'(T^*) = 1$.

If $q > q_2$, then there is a supercritical flip BCB for G^2. As T is increased and passes through T^*, an attracting 2-periodic orbit of G is replaced by an attracting 4-periodic orbit of G.

The colours for the bifurcation boundaries in Figure 2 are chosen as in the previous case: brown solid line for flip supercritical, brown dashed line for flip subcritical, and red dashed line for persistence BCBs.

Other BCBs of 2-periodic cycles occur when $T = F^2(T)$, for some $T < 1$. In this case, there are fold and persistence BCBs.

When $q > q_3 \approx 0.3575$, a fold BCB for G^2 occurs when $T = F^2(T)$. The unstable 2-periodic orbit that emerged at the fold SB collides with the attracting 2-periodic orbit of F and both disappear. The value q_3 is found solving (numerically) system $(f \circ F)(T) = T$, $(f \circ F)'(T) = 1$. The bifurcation boundary for this fold BCB is represented by a green curve in Figure 2 (for a zoom, see Figure 3 (b)). At $(T, q) = (\tilde{T}, q_3) \approx (0.5709, 0.3575)$, the boundaries of the fold SB and the fold BCB collide.

For $q < q_3$, a persistence BCB for G^2 occurs when $T = F^2(T)$. We distinguish two cases. If $q_3 > q > q_4 \approx 0.0637$, then this persistence BCB is observable: as T increases or q decreases and meets the bifurcation boundary, the 2-periodic orbit of F becomes virtual and it is replaced by a 2-cycle $\{p_1, p_2\}$ with $p_1 = f(F(p_1))$. For $q < q_4$, the 2-periodic orbit of F is unstable, and the persistence BCB is non-observable.

Bifurcation boundaries for persistence BCBs are represented by red curves in Figure 2; the trace is continuous for the observable case, and discontinuous for the non-observable one.

3.2.3. BCBs of 4-periodic cycles

Finally, we briefly discuss the possible border-collision bifurcations for G^4. There are four possibilities:

- First, let $T \approx 1.904$ be the largest value of T for which $f^4(T) = T$ holds. At this point, there is a persistence BCB for the bifurcation parameter T, which is observable: as T decreases, the admissible 4-periodic attractor of f becomes virtual and it is replaced by an admissible attracting cycle $\{p_1, p_2, p_3, p_4\}$ of G, satisfying $G^4(p_4) = F(f^3(p_4)) = p_4$. The corresponding bifurcation boundary $T = T_4$ is represented by a red solid vertical line in Figure 2.
- Let us now choose, for each $q \in (0, 1)$, the smallest T such that $F^4(T) = T$ holds. This expression defines a new (observable) fold BCB. The same occurs for those values $T < 1$ such that $(f \circ F)^2(T) = T$, $T < 1$.
- Finally, values $T > 1$ such that $(F \circ f)^2(T) = T$ give rise to either persistence or fold BCBs for G^4, depending on if $T > \overline{T}$ (fold) or $T < \overline{T}$ (persistence), where $\overline{T} \approx 1.6534$ was defined in Subsection 3.1. As before, the bifurcation boundary for the fold BCB is represented in Figure 2 by a green solid line, and the persistence BCB by a red solid line.

We have not included all persistence BCBs of 4-periodic cycles in Figure 2 to avoid complicating too much the diagram.

4. Numerical bifurcation diagrams

It is worth emphasizing that the bifurcation analysis made in the previous section allows us to split the parameter plane (T, q) into five different regions: two bistability regions and three regions where (3) with $r = 2.6$ has a unique periodic attractor, with period 1, 2 or 4, respectively. See Figure 2(b).

In particular, we see that the limit cases are robust in the following sense: for small enough values of T, the dynamics of (3) are similar to the dynamics of PH (limit case $T = 0$), while for large enough values of q (q close to 1), the dynamics of (2) are similar to those of TH (limit case $q = 1$). In both cases, a sequence of period-halving bifurcations stabilizes the positive equilibrium as harvesting intensity increases (increasing the harvesting proportion q in PH or decreasing the threshold T in TH). In the first case, the flip bifurcations are smooth, whereas in the second one they are border-collision bifurcations. In Figure 4(a), we show the bifurcation diagram of (3) for $T = 0.1$, which is similar to the usual bifurcation diagram for PH (see, e.g. [14, Figure 2]l), but extinction is not possible due to the minimum biomass level ensured by the threshold harvesting rule. In Figure 4(b), we show the bifurcation diagram of (3) for $q = 0.9$, which is qualitatively analogous to the bifurcation diagram for TH [10, Figure 3].

Next we illustrate the dynamics for other values of the parameters, showing the most relevant phenomena.

When q is the bifurcation parameter, some numerical bifurcation diagrams were plotted by Franco and Perán in [8]. Our results allow us to explain in detail the main changes in the dynamics of (3) as q is smoothly varied, for a fixed value of T.

We illustrate the dynamics with two cases in Figure 5. The bifurcation diagram for $T = 0.75$ is shown in Figure 5 (*a*). Although increasing q is stabilizing, bistability is another outcome. More precisely, there are three smooth bifurcations and one border-collision

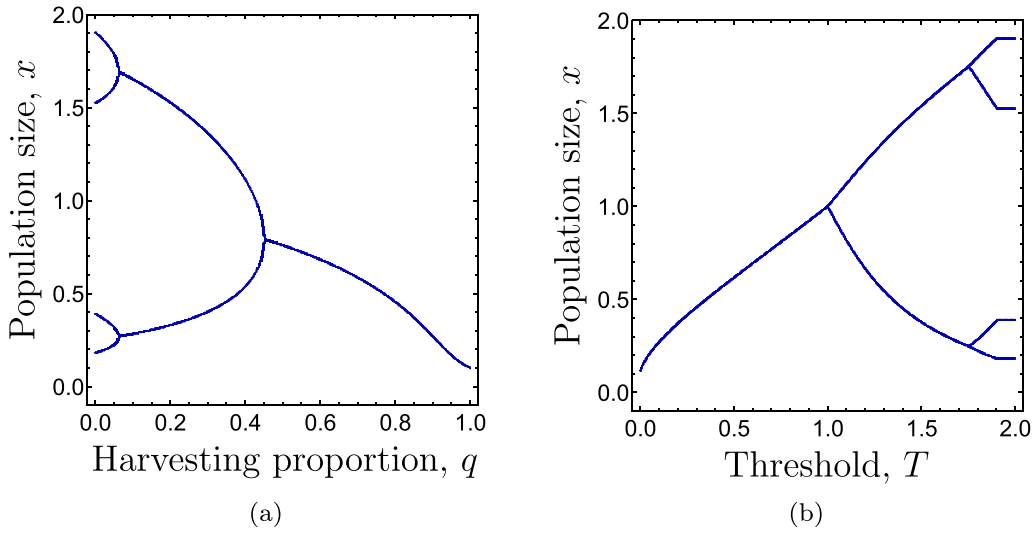

Figure 4. Bifurcation diagrams for (3) with $r = 2.6$. (a) $T = 0.1$ and bifurcation parameter q. (b) $q = 0.9$ and bifurcation parameter T.

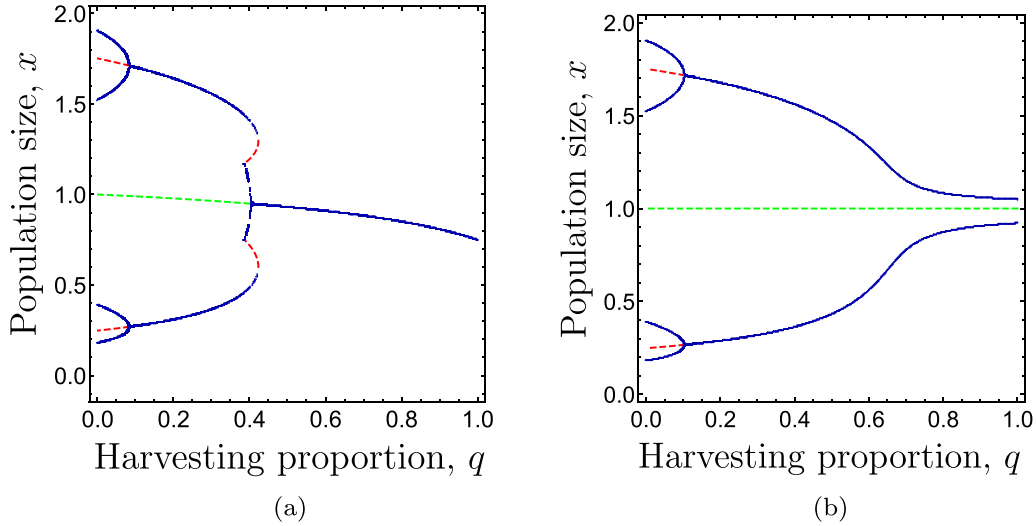

Figure 5. Bifurcation diagrams for (3) with $r = 2.6$ and bifurcation parameter q. In both cases, the green dashed line represents an unstable fixed point of G, and red dashed lines correspond to unstable 2-cycles. (a) $T = 0.75$. (b) $T = 1.05$. (Colours refer to the online version).

bifurcation. A first flip SB occurs at $q = q_1 \approx 0.083$, at which the 2-periodic orbit of G becomes asymptotically stable. At $q = q_2 \approx 0.386$, $F^2(T) = T$, and there is a fold BCB for G^2. After a new flip SB at $q = q_3 \approx 0.403$, the stable 2-cycle arising from the fold BCB disappears, and the positive fixed point p of F becomes asymptotically stable. Finally, at $q = q_4 \approx 0.423$, the unstable 2-cycle arising from the fold BCB collides with the stable 2-cycle of G and both disappear through a fold SB for G^2. Bistability occurs for $q \in (q_2, q_4)$, corresponding to regions B_2 $(q_2 < q < q_3)$ and B_1 $(q_3 < q < q_4)$ in Figure 3(a). Our numerical experiments suggest that p is a global attractor for $q > q_4$. As q tends to 1, p approaches $T = 0.75$, which is indeed a global attractor in the limit case $q = 1$, where PTH becomes TH, see [10].

For $T = 1.05$, the bifurcation diagram is shown in Figure 5(b). The only bifurcation occurs at $q \approx 0.103$, and it is a flip SB, at which the 2-periodic orbit of G becomes asymptotically stable. As $q \to 1$, the attracting 2-cycle approaches $\{T, f(T)\}$, which is the attractor of TH in the limit case $q = 1$. Here, $T = 1.05, f(T) \approx 0.922$.

When T is the bifurcation parameter, several bifurcation diagrams are shown in [9, Figure 6]. Our results in Subsections 3.1, 3.2.1 and 3.2.2 provide a theoretical framework to rigorously explain those diagrams.

An interesting result from [9] is that period-halving bifurcations cannot stabilize a positive equilibrium of (3) as a result of increasing harvesting intensity by decreasing the threshold from $T = 1$. However, our results in this paper reveal that period-halving bifurcations can stabilize a 2-periodic orbit when the threshold gets smaller. Moreover, two stability switches can occur for some values of the harvesting proportion q. See Figure 6 (a).

Other interesting bifurcation scenario occurs when, for a fixed value of q, a continuous variation of the parameter T passes through the bistability region labelled as B_4 in Figure 3(b). For example, if we choose $q = 0.185$, then the attracting 2-periodic orbit of (3) with $r = 2.6$ first undergoes a period-doubling SB at $T = T_1 \approx 1.653$. A fold SB at $T = T_2 \approx 1.683$ gives rise to a pair of 4-cycles (one attracting and one repelling). The unstable 4-cycle collides with the attracting 4-cycle born at the flip SB and both disappear after a

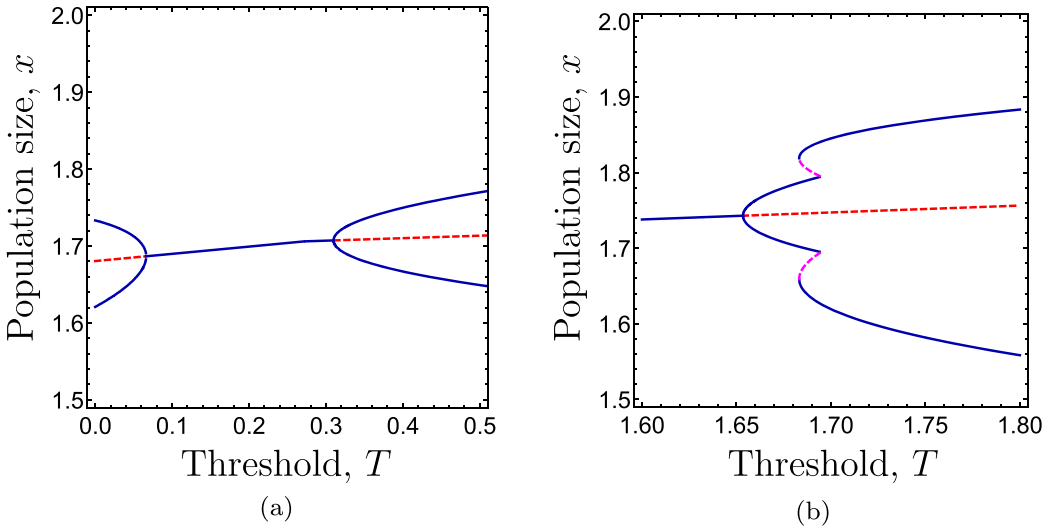

Figure 6. Detail of the upper branch of the bifurcation diagram for (3) with $r = 2.6$. Red dashed lines correspond to unstable 2-cycles, and magenta dashed lines to unstable 4-cycles. (a) $q = 0.06$ and bifurcation parameter $T \in (0, 0.5)$, showing two consecutive flip smooth bifurcations (4-cycle $\to$ 2-cycle $\to$ 4-cycle). (b) $q = 0.185$ and $T \in (1.6, 1.8)$, showing two smooth bifurcations (flip and fold) and one-fold BCB for G^4. (Colours refer to the online version).

fold BCB for G^4 occurs at $T = T_3 \approx 1.695$, for which $G^4(T_3) = T_3$. For $T \in (T_2, T_3)$, there is bistability between two 4-cycles of G. The upper branch of the corresponding bifurcation diagram is shown in Figure 6(b).

As far as we know, the consequences of persistence BCBs have not been studied for model (3). We illustrate such effects choosing $q = 0.35$. An observable persistence BCB for G^2 occurs at $T = T_1 \approx 0.548$, where $F^2(T_1) = T_1$, and a non-observable persistence BCB for G occurs at $T = 1$. The observable/non-observable character is clear in Figure 7(a), where we show the bifurcation diagram (blue colour) together with the average population size (magenta colour). The effect is even more evident in Figure 7(b), where we show the average population size (magenta line) and the positive equilibrium of G (black dashed line). As T is increased from $T = 0$, the average population size is bigger than the equilibrium, but this tendency begins to change at $T = T_1$. No effect is observed in the average population size at $T = 1$, where the positive equilibrium stops increasing and becomes constant.

5. Discussion

Our main aim in this paper was providing a deeper analysis of the dynamics and bifurcations in discrete single-species population models subject to proportional threshold harvesting by using the theory of piecewise-smooth one-dimensional maps [2,6]. Our purpose choosing the Ricker map $f(x) = xe^{r(1-x)}$ with $r = 2.6$ as a case study was twofold. On the one hand, the same example was used for related harvesting rules in the recent literature; in particular, for threshold harvesting in [10] and for constant-catch threshold harvesting in [15]. This allows us to compare the obtained results and to understand the typical dynamical features of each different threshold rule. On the other hand, the relatively simple dynamics of the unharvested model (having an attracting 4-periodic orbit) allowed

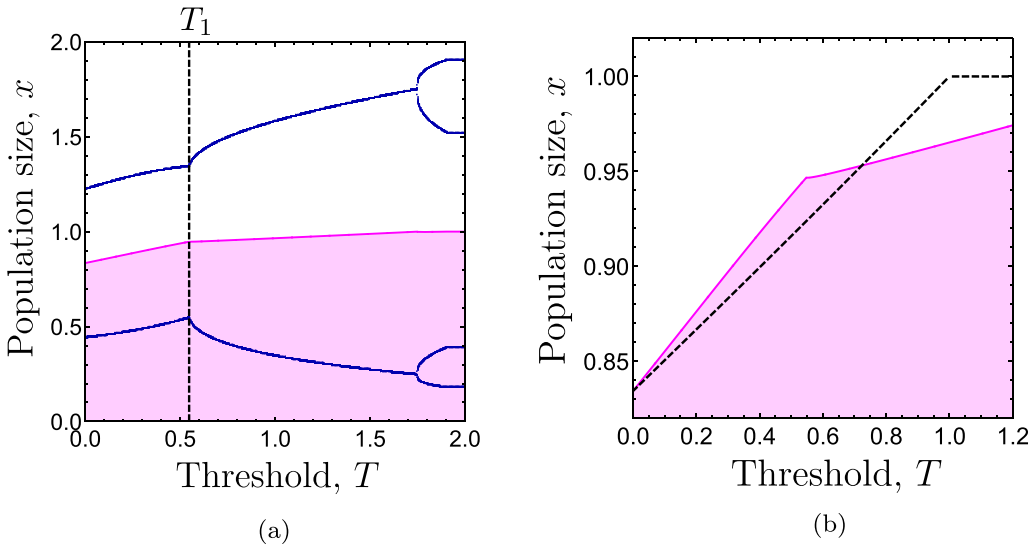

Figure 7. Illustration of the consequences of observable and non-observable persistence BCBs in model (3). The magenta line, emphasized by the shadowed region below it, represents the average population size for each value of the threshold level. (a) Bifurcation diagram for (3) with $r = 2.6$, $q = 0.35$ and bifurcation parameter T. The average population size is also shown. At $T = T_1 \approx 0.548$, a persistence BCB occurs. (b) Average population size (magenta) together with the positive equilibrium of G (black dashed lines) to emphasize the influence of observable and non-observable persistence BCBs (see the text). (Colours refer to the online version).

us to arrive at a thorough picture of the global dynamics depending on the two relevant parameters from a management point of view.

In comparison with the above-mentioned threshold rules, the main feature of proportional threshold harvesting is that the map G governing this rule (see Equation (2)) does not have flat intervals leading to superstable attractors. For this reason, some new phenomena appear; for example, we emphasize the possibility of subcritical flip border-collision bifurcations as the threshold passes the critical value $T = 1$. We also point out the relevant difference between observable and non-observable persistence bifurcations, which, as far as we know, has not been reported before. Even if an observable persistence bifurcation does not change essentially the dynamics because the period of the attractor remains the same and no other periodic points are created or destroyed, the non-smooth character of the bifurcation can explain dramatic changes in the rate of change of population average, as Figure 7 illustrates.

Finally, we emphasize that the PTH rule defined by Equation (2) is a 'precautionary' threshold harvesting strategy in the spirit of [7]. This means that, even after harvesting, population stock cannot fall below the threshold level. One important consequence is that the map G defining the between-year dynamics of the exploited population is continuous. This is contrast with other threshold rules, which lead to piecewise continuous maps, thus exhibiting more complicated bifurcation scenarios (see [3,11]).

Acknowledgments

The author thanks two anonymous reviewers for their constructive and useful comments, and for pointing out some references.

Disclosure statement

No potential conflict of interest was reported by the author.

Funding

The author acknowledges the support of the research Grant Number MTM2017–85054–C2–1–P (AEI/FEDER, UE)

ORCID

Eduardo Liz http://orcid.org/0000-0003-1975-5182

References

[1] Z. AlSharawi and M.B. Rhouma, *The Beverton-Holt model with periodic and conditional harvesting*, J. Biol. Dyn. 3 (2009), pp. 463–478.
[2] V. Avrutin, L. Gardini, I. Sushko, and F. Tramontana, *Continuous and Discontinuous Piecewise-Smooth One-Dimensional Maps: Invariant Sets and Bifurcation Structures*, World Scientific Series on Nonlinear Science, vol. 95, World Scientific, Singapore, 2019.
[3] G.I. Bischi, F. Lamantia, and F. Tramontana, *Sliding and oscillations in fisheries with on-off harvesting and different switching times*, Commun. Nonlinear Sci. Numer. Simul. 19 (2014), pp. 216–229.
[4] C.W. Clark, *Mathematical Bioeconomics: The Mathematics of Conservation*, 3rd ed., John Wiley & Sons Inc., Hoboken, NJ, 2010.
[5] J.J. Deroba and J.R. Bence, *A review of harvest policies: understanding relative performance of control rules*, Fish. Res. 94 (2008), pp. 210–233.
[6] M. di Bernardo, C.J. Budd, A.R. Champneys, and P. Kowalczyk, *Piecewise-smooth Dynamical Systems: Theory and Applications*, Applied Mathematical Sciences, vol. 163, Springer-Verlag, London, 2008.
[7] K. Enberg, *Benefits of threshold strategies and age-selective harvesting in a fluctuating fish stock of Norwegian spring spawning herring Clupea harengus*, Mar. Ecol. Prog. Ser. 298 (2005), pp. 277–286.
[8] D. Franco and J. Perán, *Stabilization of population dynamics via threshold harvesting strategies*, Ecol. Complex 14 (2013), pp. 85–94.
[9] F.M. Hilker and E. Liz, *Proportional threshold harvesting in discrete-time population models*, J. Math. Biol. 79 (2019), pp. 1927–1951.
[10] F.M. Hilker and E. Liz, *Threshold harvesting as a conservation or exploitation strategy in population management*, Theor. Ecol. 13 (2020), pp. 519–536.
[11] F.M. Hilker and C. Lois-Prados, *Bifurcation sequences in a discontinuous piecewise-smooth map combining constant-catch and threshold-based harvesting strategies*, Submitted, 2021.
[12] M. Kot, *Elements of Mathematical Ecology*, Cambridge University Press, New York, 2001.
[13] R. Lande, B.E. Sæther, and S. Engen, *Threshold harvesting for sustainability of fluctuating resources*, Ecology 78 (1997), pp. 1341–1350.
[14] E. Liz and F.M. Hilker, *Harvesting and dynamics in some one-dimensional population models*, in *Theory and Applications of Difference Equations and Discrete Dynamical Systems*, Z. AlSharawi, J. Cushing, and S. Elaydi, eds., Springer. Proceedings in Mathematics & Statistics, Vol. 102, Springer-Verlag, Berlin, 2014, pp. 61–73.
[15] E. Liz and C. Lois-Prados, *Dynamics and bifurcations of a family of piecewise smooth maps arising in population models with threshold harvesting*, Chaos 30 (2020), pp. 073108. (17 pp.).
[16] D. Ludwig, *Management of stocks that may collapse*, Oikos 83 (1998), pp. 397–402.
[17] P.M. Mace, *Relationships between common biological reference points used as thresholds and targets of fisheries management strategies*, Can J. Fish. Aquat. Sci. 51 (1994), pp. 110–122.

[18] T.J. Quinn II and R.B. Deriso, *Quantitative Fish Dynamics*, Oxford University Press, New York, 1999.
[19] T.J. Quinn II, R. Fagen, and J. Zheng, *Threshold management policies for exploited populations*, Can J. Fish. Aquat. Sci. 47 (1990), pp. 2016–2029.
[20] H.R. Thieme, *Mathematics in Population Biology*, Princeton Series in Theoretical and Computational Biology, Princeton University Press, Princeton, NJ, 2003.